Time Series Measurements from a Moored Fluorescence-Based Dissolved Oxygen Sensor

RICHARD E. THOMSON AND TERRENCE A. CURRAN

Institute of Ocean Sciences, Sidney, British Columbia, Canada

M. COREEN HAMILTON AND RONALD MCFARLANE

Seastar Instruments, Ltd., Sidney, British Columbia, Canada

(Manuscript received 4 August 1987, in final form 30 December 1987)

ABSTRACT

We present an analysis of time-series measurements from a prototype fluorescence-quenching dissolved oxygen sensor moored for a six-day period in late March 1987 at 100 m depth in Saanich Inlet, British Columbia. Temporal variations in dissolved oxygen are shown to be consistent with concomitant variations in water properties obtained from a moored Aanderaa RCM4 current meter and daily vertical profiles. Results suggest that fluorescence-based instrumentation have sufficient resolution and stability for a variety of mooring and profiling applications involving the measurement of dissolved oxygen concentration.

1. Introduction

Temperature, salinity and dissolved oxygen concentration are primary scalar properties needed to characterize the physical structure of marine and freshwater environments. Although it is not a conservative property, dissolved oxygen serves as a valuable tracer for mixing and ventilation throughout the water column and is a key index of water quality in regions of significant biological oxygen demand. Measurements of dissolved oxygen content are used to delineate oceanic water masses, to estimate the timing and intensity of upwelling processes along continental margins, and to establish the occurrence of deep water renewal events in coastal fjords. When water bottle sampling was the sole method for comprehensive investigation of water property variability, the measurement of dissolved oxygen was only slightly more arduous and time-consuming than the measurement of temperature and salinity. The advent of the modern CTD, with its rapid O (0.1 s) temperature and conductivity response, has altered this situation considerably and has emphasized the requirement for a rapid response dissolved oxygen probe.

At present, two techniques are used for in situ measurement of dissolved oxygen content: Water bottle (hydro) sampling followed by chemical "pickling" and end-point titration (Strickland and Parsons 1968; Hitchman 1978); and electronic sampling using a membrane-covered polarographic "Clark" cell (Clark U.S. Patent No. 2 913 386; Hitchman 1978; Langdon 1984). Water bottle sampling is based on the Winkler method of dissolved oxygen determination and is considered accurate to 1% provided that the chemical analysis methods are rigidly applied. During the "pickling" step of the Winkler method, the dissolved oxygen in the hydro sample oxidizes Mn(II) to Mn(III) in alkaline solution to form a precipitate of MnO_2. This is followed by oxidation of added I^- by the Mn(III) in acidic solution. The resultant I_2 is titrated with thiosulfate solution using starch as an endpoint indicator. Principal drawbacks to the technique are its limitation to discrete depths and the inability to use the method in moored or real-time profiling configurations. In addition, the collection and titration of water samples tends to be labor intensive and slow. Erroneous data can result if air bubbles become entrapped in the sample during collection or if samples are not pickled immediately after they are drawn.

The Clark cell operates on the basis of electro-reduction of molecular oxygen at a cathode. When used in a polarographic mode, the electric current supplied by the cathode is proportional to the oxygen concentration in the surrounding fluid. To lessen the sensitivity of the device to turbulent fluctuations in the fluid, the electrode is covered with an electrolyte and membrane. Oxygen must then diffuse down-gradient through the membrane into the electrolyte before it can be reduced at the surface of the cathode.

The basic concept of the Clark cell is clearly amenable to profiling and moored configurations. Unfortunately, there are fundamental limitations to the Clark cell that mitigate against its use as a standard rapid-response oceanographic probe. Specifically, the molec-

Corresponding author address: Dr. Richard E. Thomson, Institute of Ocean Sciences, P.O. Box 6000, 9860 West Saanich Road, Sidney, British Columbia, Canada V8L 4B2.

ular diffusion of oxygen through the boundary layer near the surface of the probe is an inherently slow process that limits the response time of the Clark cell to several minutes. Moreover, the electrochemical reaction within the cell consumes oxygen, and stirring may be required to maintain the correct external oxygen concentration. Also, physical changes in the structure of the cell (due to alterations in the diffusion characteristics of the membrane through the effects of temperature, mechanical stress and biological fouling and to deterioration of the electrolyte and the electrode surfaces) require recalibration of the Clark cell every several hours. The need for frequent recalibration complicates the use of the polarographic technique for profiling and severely limits its application as a moored instrument. A recent modification by Langdon (1984) uses a pulse technique to reduce the calibration drift. Although no field profiles or long-term deployment data were obtained, the modification was found to produce enhanced stability in laboratory tests over periods of hours for a sampling rate of ten readings per hour. The long-term stability was estimated by comparing instrument calibrations 45 days apart. No statistical difference was found in the slope or zero intercept of the calibration function. However, a long sensor response time of 3 to 5 minutes was needed for accurate results.

The use of fluorescence quenching for oxygen measurement is not a new concept. As early as the 1930s, Kautsky and Hirsch had observed and published a series of papers concerning the effect of oxygen on the luminescence of dyes on an inorganic absorbant (Kautsky 1939). The technique has numerous advantages over the Clark cell including an order of magnitude more rapid response and long-term stability. No oxygen is consumed in the process and there are no rapid changes in the physical configuration of the oxygen sensing portions of the apparatus with time. The design of a fiber-optic fluorescence-quenching probe for in vivo measurement of oxygen partial pressure in blood is described by Peterson et al. (1984) and Gehrich et al. (1986); corresponding designs for the measurement of dissolved oxygen in air and water are described by Bergman (1968), McFarlane and Liese (1984), Wolfbeis et al. (1985) and Zhujun and Seitz (1986). Preliminary results from oceanic field tests of a fluorescence-based dissolved oxygen profiler are presented by McFarlane and Hamilton (1987). From theoretical considerations, the fluorescence-based technique is at least as accurate and sensitive as the Clark Cell.

This paper has a two-fold purpose: 1) to familiarize the oceanographic and limnologic communities with fluorescence-quenching as a viable technique for the rapid sensing of dissolved oxygen concentrations, and 2) to present time-series observations from a recently developed fluorescence-based dissolved oxygen sensor moored at a depth of 100 m for a period of six days in Saanich Inlet, British Columbia. Data from the sensor are intercompared with simultaneous time-series measurements of temperature, salinity, pressure and horizontal velocity obtained from a moored current meter and with profile observations taken using a Yellow Springs Instruments (YSI) Model 57 Oxygen Meter. Although water sampling combined with the Winkler analysis method yields more precise measurements of dissolved oxygen, the YSI instrument is considerably more convenient for profiling operations. A comparison of oxygen values from the two techniques showed that the YSI instrument had sufficient accuracy for initial field testing of the new fluorescence-based sensor.

2. Instrument operation and design

a. Basic concepts

The present device is based on the principle that the fluorescence intensity of an externally excited fluorophore will be attenuated ("quenched") in direct relation to the concentration of dissolved oxygen (an acceptor molecule) in an ambient fluid. If a pulse of light of suitable wavelength is directed at a bulk fluorophore, the excited molecules de-excite with time, t, at an e-folding rate

$$K = K_E + K_I + K_T \cdot [C]$$

in which $[C]$ is the concentration of the acceptor molecules in the bulk fluorophore and where K_E, K_I and K_T are the respective time constants for the emission of a photon, the internal conversion of the excitation energy and the transfer of energy to an acceptor molecule within the fluorophore (Berlman 1971). The number of remaining excited molecules, N, after a given time is then $N = N_0 \exp(-Kt)$ where N_0 is the number of excited fluorophore molecules created by the initial light pulse.

Suppose we now define Q (the fluorescence quantum yield) as the ratio of the number of photons emitted by the fluorophore to the number of excitation photons absorbed by the fluorophore such that

$$Q = K_E/(K_E + K_I + K_T \cdot [C]).$$

It can then be shown (cf. McFarlane and Hamilton 1987) that the ratio of the fluorescence quantum yield in the absence of oxygen ($[C] = 0$) to the fluorescence quantum yield in the presence of dissolved oxygen, Q_0/Q, is given by

$$Q_0/Q = 1 + \tau K_T \cdot [C] \quad (1a)$$

in which

$$\tau = 1/(K_E + K_I) \quad (1b)$$

is a measure of the modified time response due to the presence of acceptor (oxygen) molecules. The case $Q = 1$ implies that fluorescence is the sole contributor to the de-excitation process ($K_I = K_T = 0$). The Stern-

Volmer equation (1a) can also be written in terms of the corresponding fluorescence intensities

$$I_0/I = 1 + \tau K_T \cdot [C]$$

where I_0/I is the response measured by the fluorescence-based oxygen sensor.

b. *Instrument description*

The optical system of the fluorescence-based dissolved oxygen sensor is presented in Figure 1a. Because the source light produced by the zenon-flash bulb is broadband, the light is first passed through an interference filter which transmits only the excitation wavelength of the sensing chemical (fluorophore). The excitation light is then collimated and passed through a dichroic beam-splitter. Approximately 4% of the excitation light is reflected by the dichroic beam-splitter towards a reference detector. The remaining portion of the light is focused onto the end of an optical fiber and subsequently excites the fluorophore at the opposite end of the fiber link. Fluorescent light emitted by the sensing chemical is then transmitted back along the fiber. Light emerging from the fiber is collimated and reflected by the dichroic beam-splitter towards a photomultiplier tube. Prior to reaching the photomultiplier tube, the light is directed through a second interference filter to remove background ambient light.

A schematic layout of the dissolved oxygen sensor is presented in Fig. 1b. The operation of the xenon flash, photomultiplier tube, and reference detector are coordinated by the microcomputer, which can be programmed to run autonomously for moored operations or interactively for profiling operations. Batteries supply power to the device during moored configurations. The optical system, electronics and batteries are contained within the pressure case. The sensing end of the optical fiber is mounted outside the pressure case and connected to the interior electronics via a waterproof fitting. Underwater connectors allow a user to interact with the instrument via a computer terminal.

The signal from the photomultiplier tube and the reference detector are digitized by the microcomputer system and then averaged over a specified number of flashes. The averaged signal from the photomultiplier tube is divided by the averaged reference detector signal to produce a "reading". By altering the flash rate and sequencing scheme, the sampling rate can be varied from one reading every second to one reading every two hours. Further details on the data-recording procedure are presented in the next section.

c. *Instrument response*

Measurements obtained in the laboratory indicate that the response time of the sensor is 1 second in air and 10 seconds in water. However, this difference could be an artifact of the laboratory testing system since the near similarity between profiles taken at different drop rates suggest that actual oceanic response time may be

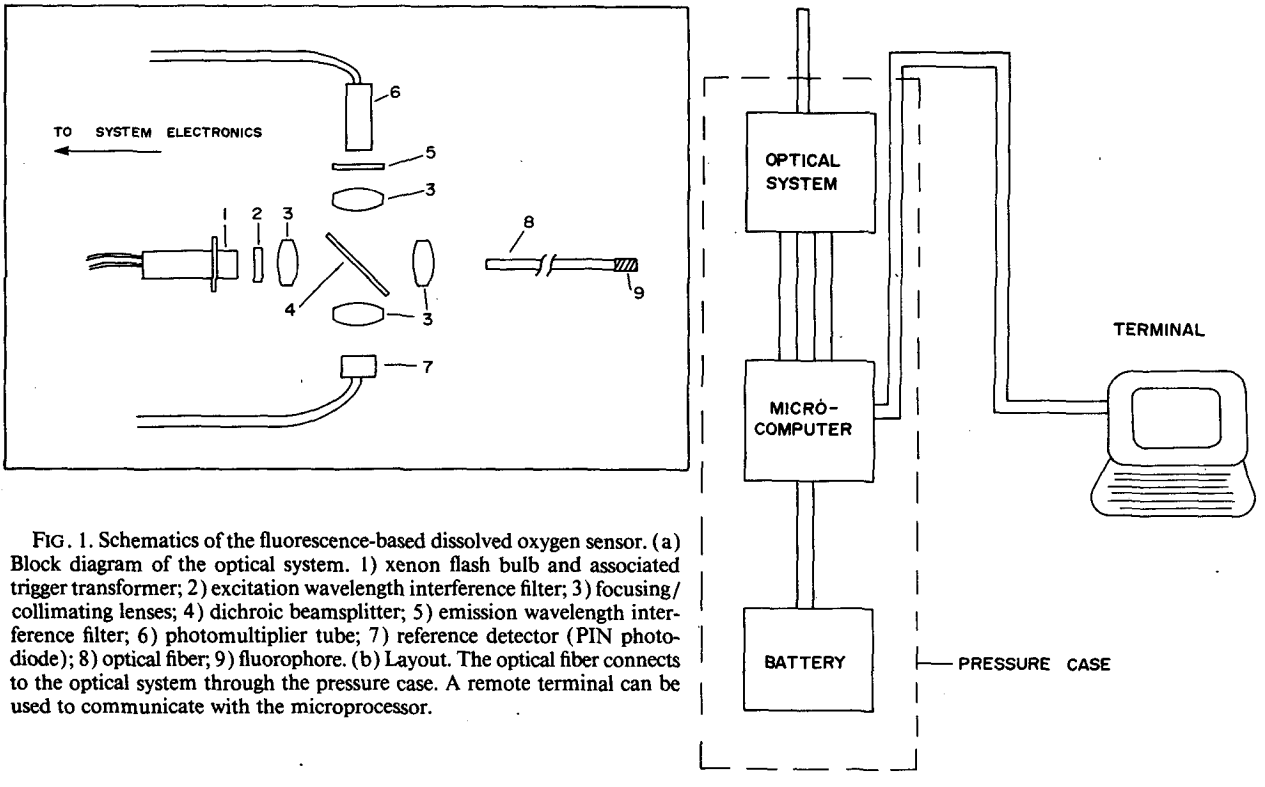

FIG. 1. Schematics of the fluorescence-based dissolved oxygen sensor. (a) Block diagram of the optical system. 1) xenon flash bulb and associated trigger transformer; 2) excitation wavelength interference filter; 3) focusing/collimating lenses; 4) dichroic beamsplitter; 5) emission wavelength interference filter; 6) photomultiplier tube; 7) reference detector (PIN photodiode); 8) optical fiber; 9) fluorophore. (b) Layout. The optical fiber connects to the optical system through the pressure case. A remote terminal can be used to communicate with the microprocessor.

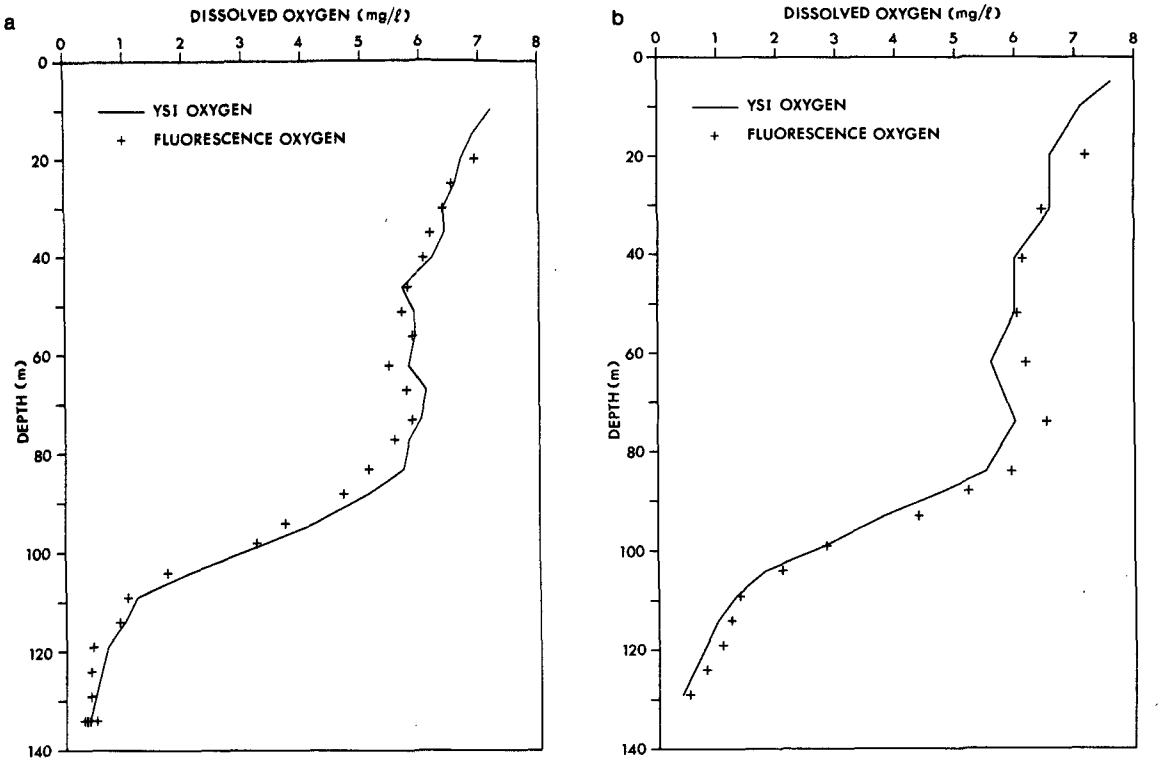

FIG. 2. Dissolved oxygen profiles obtained by the fluorescence-based sensor (+) and YSI sensor (solid line) in Saanich Inlet on 13 February 1987. The respective fluorescence-based and YSI values were taken 10 s and 2 min after the probe reached the specified depth. (a) Descent and (b) ascent.

closer to 1 s. One of the impediments to determination of a more precise response time is the 0.07 mg l^{-1} noise level of the sensor. Although instrument modifications are underway to eliminate this problem, the noise level presently limits the instrument sensitivity and therefore its ability to distinguish rapid O (1 s) changes in dissolved oxygen level. Regardless of the exact value, a response time of 1 to 10 seconds is acceptable in most profiling operations requiring vertical spatial resolutions of 1 to 10 m.

The ability of the fluorescence-based sensor to reproduce dissolved oxygen profiles was demonstrated during a series of field trials conducted a month prior to the mooring deployment. In these tests, the prototype sensor was lowered with a YSI (Clark Cell) probe to the bottom of Saanich Inlet and detailed oxygen measurements made on the up and down portions of the cast. Results for the 13 February 1987 comparison are shown in Fig. 2. Oxygen values from the YSI sensor were obtained two minutes after the instrument package was stopped at a given depth; corresponding values for the fluorescence-based sensor were taken ten seconds after the package reached depth. The shapes of the two profiles are nearly identical and, with exception of the observations taken above the oxycline on the ascent portion of the cast (Fig. 2b), show comparatively little difference in magnitude. The fact that the two curves track one another on the downcast when remnant wake effects from the probe were minimal is particularly encouraging. On the upcast, remnant turbulent mixing and vortex shedding from the probe presumably distorted the dissolved oxygen profile, causing the somewhat greater spread in values.

Finally, our laboratory tests show that high concentrations of other water dissolved fluorescing substances, such as crude oil and kraft pulp-mill effluent, do not affect the sensor response. Moreover, the choice of wavelength for the system is not dictated by the presence of other fluorescing substances.

3. Observations

Data presented in this study cover the period 26 March to 1 April 1987 and are from a site centered at 48°39.8′N, 123°30.0′W located in approximately 175 m of water at the northern end of Saanich Inlet, British Columbia (Fig. 3). Site selection was based on the close proximity to the Institute of Ocean Sciences (IOS) and on the availability of detailed background information on the regional water property structure (e.g., Herlinveaux 1962; Anderson and Devol 1973; Pickard 1975; Stucchi and Giovando 1984). Saanich Inlet is a relatively quiescent, weakly estuarine regime consisting of a deep (~200 m) north–south oriented basin separated from tidally active channels to the north by a shallow (<75 m) sill. During March and April, the inlet is

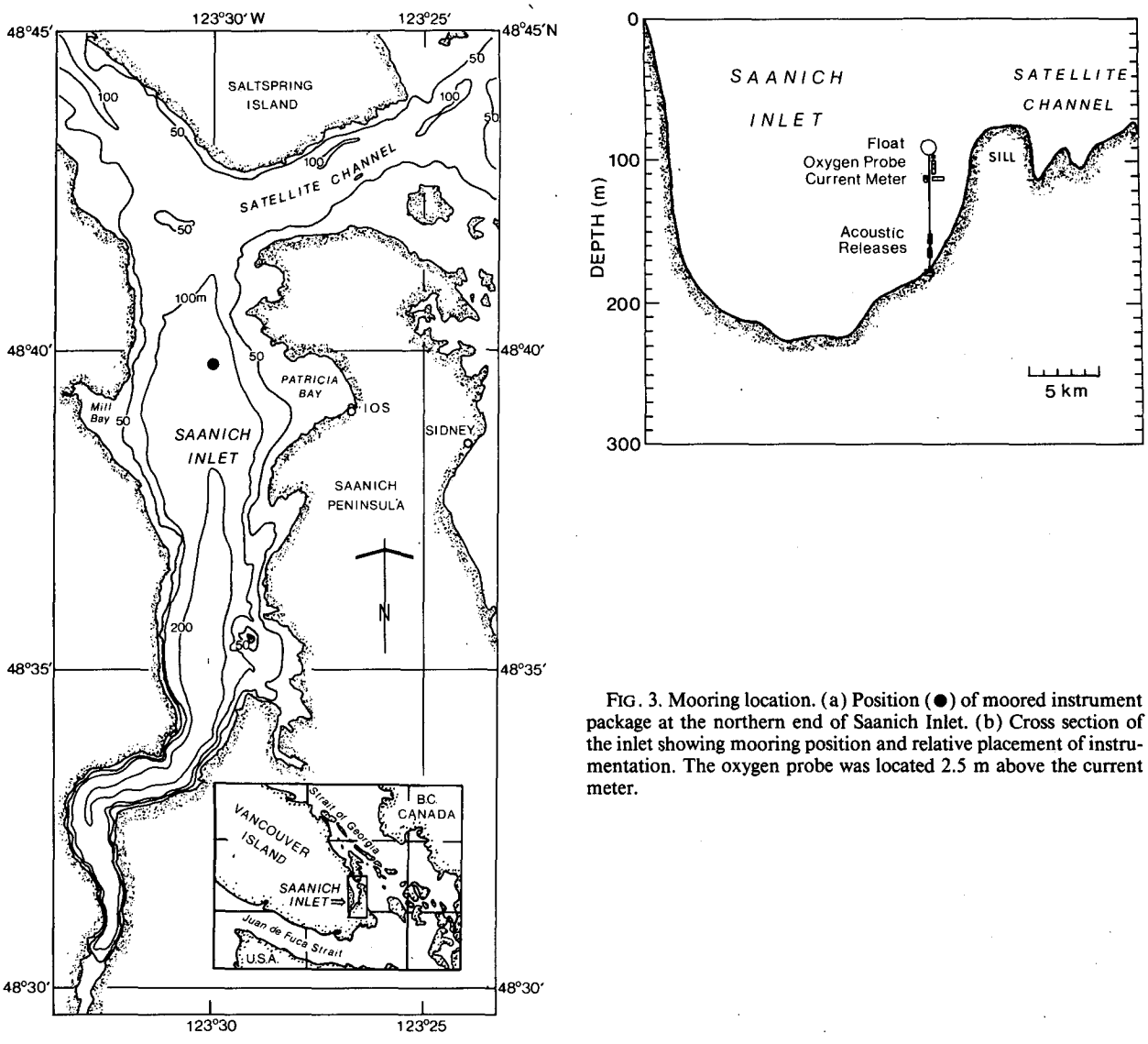

FIG. 3. Mooring location. (a) Position (●) of moored instrument package at the northern end of Saanich Inlet. (b) Cross section of the inlet showing mooring position and relative placement of instrumentation. The oxygen probe was located 2.5 m above the current meter.

weakly stratified with temperature and salinity increasing with depth below the upper few tens of meters (Herlinveaux 1962). Dissolved oxygen concentrations are typically around 5 to 10 mg l^{-1} in the upper 50 m but decrease rapidly to zero below the depth of the permanent oxycline centered near 100 m. Throughout much of the year the deeper portions of the main basin are characterized by anoxic bottom water comprised of significant levels of hydrogen sulphide. The circulation within the inlet consists of mixed, predominantly semidiurnal tidal currents with maximum speeds of order 10 cm s^{-1} superimposed on a weak estuarine flow.

a. Profile observations

Daily profiles of temperature, salinity and dissolved oxygen were obtained each morning (around 0930 local time) near the mooring site throughout the observational period using an Applied Microsystems STD/12 in combination with a YSI Model 57 Oxygen Meter. The respective accuracies of these instruments are ±0.02°C, ±0.03 ppt, ±0.1% full scale pressure (here, ±0.25 m) and ±0.10 mg l^{-1}. Owing to the relatively slow response time of the Clark cell used in the YSI probe, the profiling package had to be lowered to discrete depths and allowed to equilibrate for several minutes for each reading. Therefore, with the exception of the STD cast immediately prior to the mooring deployment, detailed information on the vertical water property structure is confined to a 40 m depth range centered at the depth of the moored instrumentation.

The vertical distributions of water properties obtained prior to the mooring emplacement (Fig. 4) closely resemble those seen in previous early spring surveys of Saanich Inlet. (Low salinity values of around 25 ppt within the upper few meters are not plotted.) In particular, we observe a gradual increase in tem-

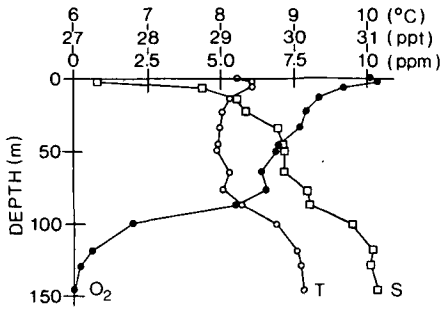

FIG. 4. Profiles of water properties taken at the mooring site several hours before deployment. For consistency, temperatures and salinities are plotted only at the depths of the oxygen measurements.

perature and salinity above sill depth followed by a more rapid increase to the top of the lower layer at around 120 m. Dissolved oxygen values decrease slowly above sill depth but then diminish rapidly to zero at a depth of around 145 m. To facilitate the data analysis, the moored instrumentation was deployed at a normal depth of 100 m commensurate with the zone of near uniform temperature and oxygen gradients.

Composite plots of temperature, salinity and dissolved oxygen concentrations for the depth range of 80 to 140 m are presented in Fig. 5. Also plotted are least-squares linear regression lines for the closely sampled depth interval 90 to 110 m centered at the depth of the current meter and dissolved oxygen sensors. The regression lines confirm the near uniformity of the temperature and dissolved oxygen gradients at the depths of the moored instrumentation over the six-day observation period and are suggestive of weak vertical mixing below sill depth in Saanich Inlet; the considerably noisier salinity variations are presumably linked to the relatively poor resolution of the conductivity cell used in the STD. The slopes of the temperature, salinity and dissolved oxygen profiles for the depth range 90 to 110 m are calculated to be 0.28×10^{-1} °C m^{-1}, 0.39×10^{-2} ppt m^{-1} and -0.18 mg l^{-1} m, respectively; associated correlation coefficients are 0.94, 0.17 and -0.91. For the entire range 60 to 145 m in Fig. 5, regression of the salinity data yields a more reliable slope of 0.25×10^{-2} ppt m^{-1} and correlation coefficient of 0.87.

b. *Moored observations*

The time series data presented in this paper are from a single taut-wire subsurface mooring instrumented with an Aanderaa RCM4 current meter, the prototype dissolved oxygen sensor and dual acoustic releases positioned in approximately 175 m of water on the southern flank of the main sill (Fig. 3b). The mooring was deployed at 1255 (all times local) on 26 March and recovered 5.89 days later at 1040 1 April 1987. Separation between the dissolved oxygen probe and the center of the current meter was roughly 2.5 m, with the top of the current meter positioned 72.5 m above the bottom. As noted earlier, selection of the instrument depth was based on a single temperature, salinity and dissolved oxygen profile taken a few hours prior to the mooring deployment which showed the main oxycline centered near 100 m depth. Observations from the current meter consist of current speed and direction, temperature, conductivity (salinity) and pressure every 5 minutes. Dissolved oxygen measurements were obtained every 10 minutes.

According to the manufacturer's specifications, the standard temperature, salinity and (500 psi) pressure sensors used in the Aanderaa current meter have respective accuracies of ±0.02°C, ±0.03 ppt and ±1%. Typical standard errors for the 500 psi (350 m) pressure sensor used in the mooring are about ±0.5 db. The threshold speed of the RCM4 is approximately 2 cm

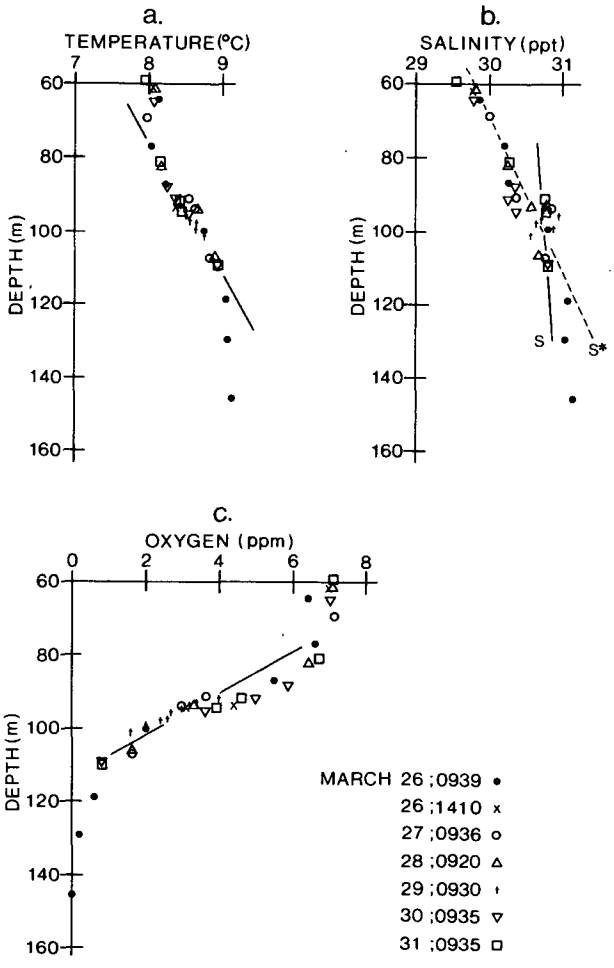

FIG. 5. Composite plots of water properties for the depth range 60 to 145 m. Symbols refer to observations on specified days. Also plotted are linear regression lines for each variable. The regression line S in (b) spans the range 90 to 110 m while the line S* spans all plotted data. $T = 5.85 + 0.0283z$ °C, $S = 30.35 + 0.00387z$ ppt ($S^* = 28.26 + 0.0247z$ ppt), $O_2 = 20.26 - 0.179z$ mg l^{-1}.

s^{-1} and speeds are accurate to ± 1 cm s^{-1} or 2% of the actual speed, whichever is greater. Directions are accurate to $\pm 5°$ for speeds in the range of 5 to 100 cm s^{-1}. With the exception of direction, which is measured instantaneously at the end of the sampling interval, all quantities derived from the current meter represent averaged values over the 5-minute sampling period. Plots of the edited time-series records are presented in Fig. 6a.

The sampling scheme for the dissolved oxygen probe is indicative of its present prototype status. First, a real-time clock in the microprocessor activates the sensor once every ten minutes. A total of eight readings are then taken, each reading being the averaged response from 16 flashes of the xenon light source. The time span for each group of eight readings is less than a minute. Because the sensor requires time to reach equilibrium ("warm-up"), the first three or four readings usually contain a degree of drift. To eliminate this drift, the first five of the eight readings are discarded. The averaged photomultiplier and reference detector signals from the last three readings are subsequently stored in nonvolatile memory. When the mooring is recovered, these stored values are downloaded onto a mainframe computer for analysis.

As with most commercially available probes (including the Clark cell), the fluorescence-based sensor actually detects the partial pressure of dissolved oxygen rather than its concentration. Calibration of the oxygen sensor therefore involves compensation for temperature and salinity in order to convert the measured oxygen levels to oxygen concentration. In the present case, the probe was first calibrated in freshwater (at approximately 13°C) in the laboratory and the slope of the

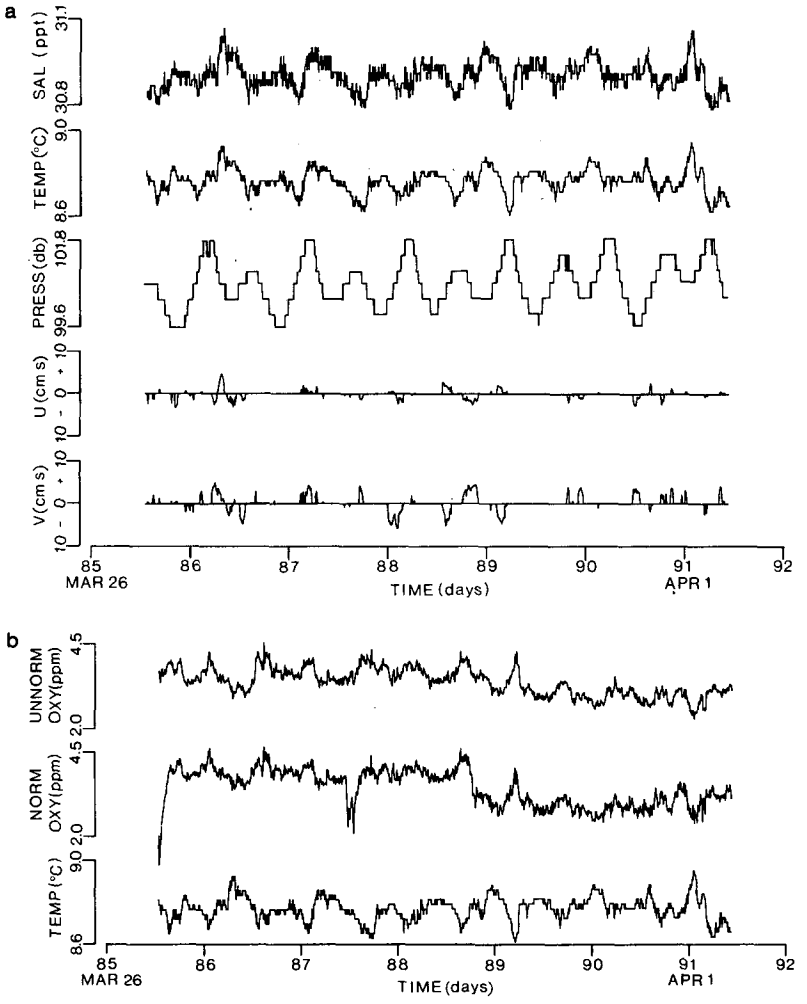

FIG. 6. Time-series records with time in Julian days 1987. (a) Five-minute records from the Aanderaa RCM4 current meter. U is positive eastward and V is positive northward. (b) Ten-minute records of unnormalized and normalized dissolved oxygen together with the 5-minute temperature records from (a).

resultant calibration plot adjusted for the average in situ temperature (8.5°C) at the probe depth over the six-day field period. This temperature-adjusted calibration is then used to convert the observed sensor values to temperature-corrected oxygen values. The observed mean value of 30.6 ppt at 100 m depth at the mooring site was used to obtain the salinity correction via the formula given in the manual for the YSI Model 57 Oxygen Meter. The depth correction for partial pressure has been ignored.

The oxygen probe records both the fluorescence signal and a reference detector value. Normalization of the fluorescence signal by the reference value is used to compensate for fluctuations in flash lamp intensity. Plots of the normalized and unnormalized records of dissolved oxygen are presented in Fig. 6b together with the temperature record from Fig. 6a. Unfortunately, the normalized record contains offsets associated with intermittent failure of the reference detector and will not be analyzed.

4. Analysis

The purpose of this section is to describe the water property variability at the mooring site in Saanich Inlet and to show that aspects of the oceanography deduced from the time series of dissolved oxygen are consistent with those obtained from the time series of temperature and salinity.

Inspection of Figures 6a and 6b reveals that property fluctuations at the mooring site are dominated by tidal period motions in the diurnal and semidiurnal bands. Temperature and salinity variations occur in-phase while temperature and dissolved oxygen variations differ in phase by roughly 180°. The mid-depth currents are weak and sporadic with northward (southward) flow marginally correlated with high (low) temperatures and low (high) oxygens. We further note that the temperature, salinity and pressure records show consistent mean and fluctuating amplitudes throughout the time series whereas the dissolved oxygen record reveals a small decrease in the mean and fluctuating oxygen levels midway through day 89. Although we cannot be certain, the latter may simply reflect a difference in the vertical and horizontal gradients of dissolved oxygen compared to other parameters (cf. Fig. 4). A slight shift in the water mass such as through current advection may have been sufficient to alter oxygen without altering temperature or salinity.

a. Basic statistics

Basic statistical properties of the edited time series records are presented in Table 1. Comparison of the composite temperature profile plotted in Fig. 5a and the mean temperature of 8.76°C listed in the table verifies that the current meter was positioned at approximately 100 m depth, consistent with the mean pressure of 100.7 db recorded by the RCM4 pressure sensor. Assuming that this is the true mean depth for the current meter, use of Table 1 and Fig. 5b suggests that mean salinity values recorded by the STD were 0.1 to 0.2 ppt less than those recorded by the current meter; similarly, mean oxygen values measured by the fluorescence-based oxygen sensor were about 0.5 mg l^{-1} greater than those measured by the YSI probe. (The mean of the normalized record is about 0.1 mg l^{-1} greater than that of the unnormalized record presented in Table 1.)

The standard deviation and range of the temperature record in Table 1 can be used in conjunction with the regression line in Fig. 5a to obtain estimates of the "effective" vertical isopycnal displacements at the depth of the moored instrumentation; i.e., changes due to horizontal and vertical motions that we interpret in terms of vertical displacements alone. Using the observed standard deviation of 0.055°C and the range of 0.272°C, together with the regression value of 0.0283°C m^{-1}, the standard deviation and range of the effective vertical isopycnal displacements are estimated to be 2.0 and 9.6 m, respectively. These displacements, together with the regression value of −0.179 mg l^{-1}/m in Fig. 5c, yield "predicted" estimates of 0.36 and 1.72 mg l^{-1} for the standard deviation and range of the dissolved oxygen signal measured by the moored oxygen probe. The actual values measured by the probe are 0.41 and 2.32 mg l^{-1}. Based on these results, it would appear that the oxygen probe yielded an accurate record of the temporal variation of dissolved oxygen at the mooring site.

Differences between the predicted and observed statistical properties are not unexpected considering the assumptions that have gone into this simple calculation, the steep gradient of the oxycline at the mooring

TABLE 1. Statistical properties of variables measured by moored instrumentation at 100 m depth in Saanich Inlet, 26 March–1 April 1987. Trends are given in specified units per day.

	Temperature (°C)	Salinity (ppt)	Oxygen (ppm)	Pressure (db)	Speed (cm s^{-1})
Mean	8.76	30.90	3.34	100.68	3.37
Std dev	0.06	0.05	0.41	0.60	0.95
Minimum	8.60	30.79	2.20	99.60	0.80
Maximum	8.94	31.06	4.51	101.80	6.50
Trend (unit day^{-1})	1.18 (10^{-5})	−2.28 (10^{-4})	−2.67 (10^{-2})	5.99 (10^{-3})	—

depth and the assumptions that have been used to calibrate the oxygen response curve of the sensor. Moreover, it is conceivable that horizontal advection contributed differentially to the temperature and oxygen observations because of respective differences in horizontal property gradients near the sill. In any case, vertical motions are expected to dominate the advectively-induced fluctuations in water properties. This is supported by the fact that horizontal gradients in water properties at 100 m are generally small (Herlinveaux 1962) and by the observation that horizontal water parcel displacements (based on the mean observed flow speed of 3.5 cm s^{-1} integrated over half a semidiurnal tidal cycle) are less than 1 km. The fact that the maximum range in pressure (2.2 m) is nearly identical to the predicted tidal range of 2.5 m for Saanich Inlet for the deployment period (Canadian Hydrographic Service 1986) indicates that mooring excursions did not contribute significantly to the observed water property fluctuations.

b. Spectral analysis

Spectra of scalar water property fluctuations derived from the Aanderaa current meter and oxygen sensor data are presented in Fig. 7. Velocity spectra are omitted since most of the 5-minute observed speeds are below threshold and therefore recorded as zeroes by the current meter. In all cases, major spectral peaks are found within the diurnal and semidiurnal tidal bands. Although the spectra roll off rapidly with frequency, ω, there are significant differences within the internal wave band $f \leqslant \omega \leqslant N$, bounded by the local Coriolis frequency, f, and the Brunt–Väisälä frequency, $N(z)$. Here, $f = 0.0626$ cph and we estimate that $N(100$

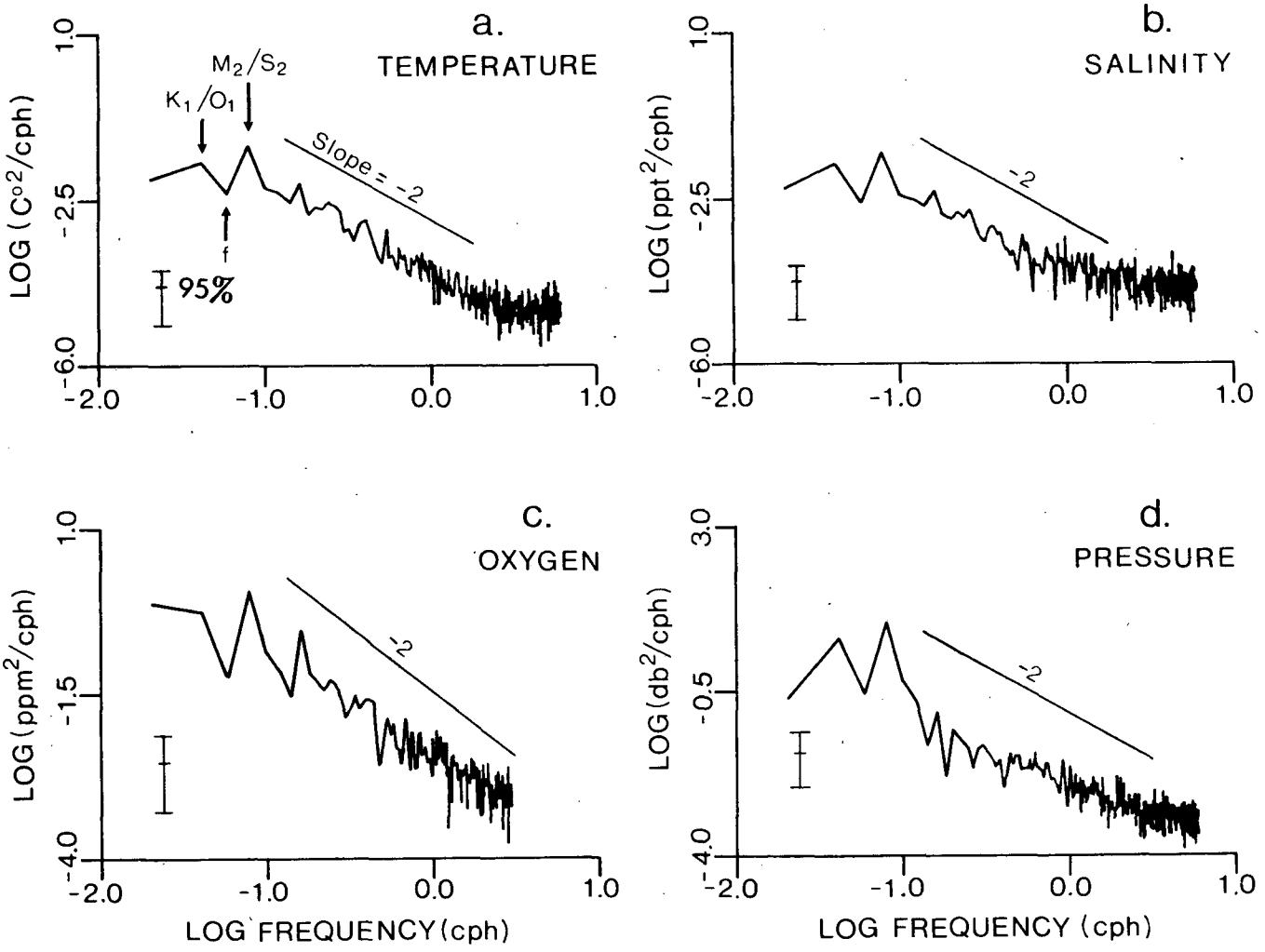

FIG. 7. Spectra of scalar water properties from moored instrumentation. Vertical bars denote 95% confidence limits based on 6 degrees of freedom per band-averaged spectral estimate. Location of major diurnal and semidiurnal frequencies and Coriolis frequency are noted in (a). The line indicates the slope for an inverse-square spectral distribution.

m) ~ 8 cph based on the linear regression lines for temperature and salinity over the range of depths presented in Fig. 5. This value for N is somewhat larger than the Nyquist frequencies of ~6 cph for the RCM4 data and 3 cph for the oxygen data.

As illustrated by Fig. 7a, temperature fluctuations within the internal wave band roughly decay as ω^{-p}, where $p = 2$ is the value proposed by Garrett and Munk (1972, 1975) for the spectrum of vertical displacements measured by moored instrumentation in the presence of isotropic internal wave motions. Flattening of the spectrum near $\log\omega = 0.5$ (3.1 cph) may be due to aliasing or to instrument noise. The fact that the Nyquist and Brunt–Väisälä frequencies are nearly coincident suggests that instrument noise is the limiting factor in resolution of the high frequency temperature oscillations. The salinity and dissolved oxygen spectra (Figures 7b, c) also decay as ω^{-2} but begin to flatten at somewhat lower frequencies than for temperature. We again conclude that instrument noise is limiting the high frequency spectral resolution. The results further indicate that the salinity and dissolved oxygen sensors achieve comparable signal resolutions but have lower resolution levels than the temperature sensor.

c. *Coherence and admittance*

Plots of coherence amplitude and phase for temperature versus salinity and temperature versus dissolved oxygen are presented in Fig. 8. The corresponding plots for admittance are presented in Fig. 8c. Only the lower portions of the frequency range are plotted since at higher frequencies the time series are essentially incoherent at the 95% confidence level (0.55). The admittances measure the amplitudes of the salinity and oxygen signals relative to the temperature signal for a given frequency band.

According to Fig. 8a, salinity and temperature are strongly coherent up to frequencies of approximately 0.45 cph (period: 2.2 h) but are essentially incoherent beyond frequencies of 0.60 cph. Within the former range, relative phases generally differ by less than 10° and the ratio of salinity-to-temperature amplitude (Fig. 8c) is about 0.85 ± 0.12 ppt °C^{-1}. Figure 8b indicates that temperature and dissolved oxygen are moderately coherent up to 0.45 cph but become incoherent for frequencies beyond 0.55 cph. Phase differences are in the range of 10° to 15° and the admittance is 6.05 ± 1.85 mg l^{-1}/°C.

The results of this section reveal that temperature and salinity fluctuations near sill depth in northern Saanich Inlet are highly correlated for periods of a few hours to a week. In contrast, temperature and dissolved oxygen fluctuations are only moderately correlated for these periods. Changes in lower layer dissolved oxygen levels may therefore be partly decoupled from local changes in density.

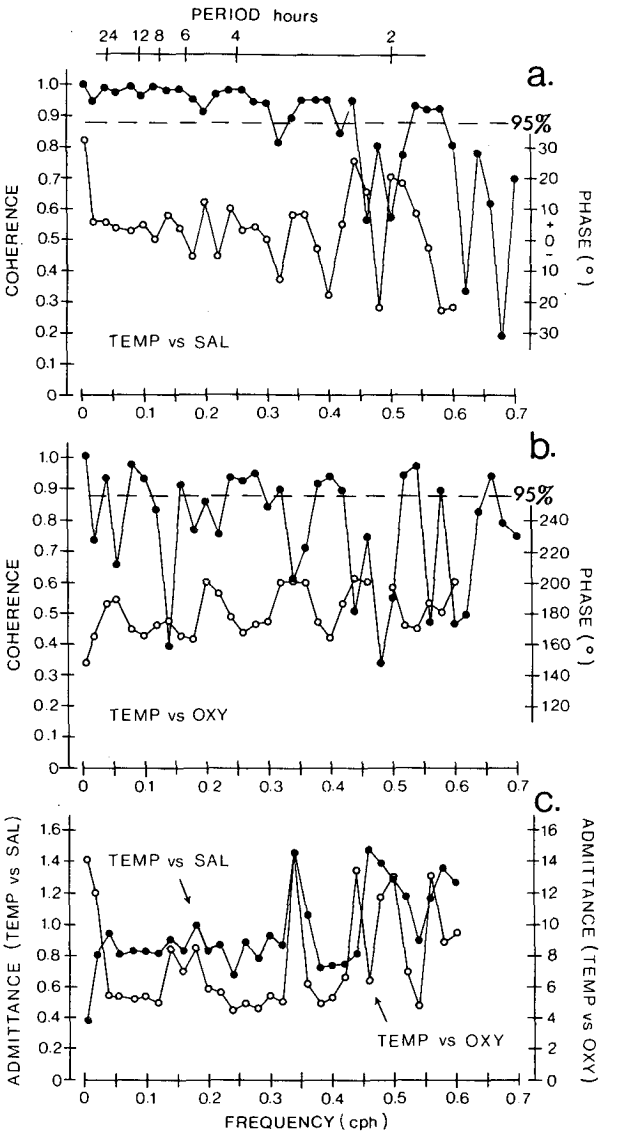

FIG. 8. (a) Coherence amplitude (solid circle) and phase (open circle) for temperature versus salinity. Horizontal line denotes the 95% confidence level. Phases for parts of the incoherent portion of the frequency range are omitted. (b) As in (a) but for temperature versus dissolved oxygen, with temperature decimated to a 10-minute sampling increment. (c) Admittances between temperature and salinity records (solid circles) and temperature and oxygen records (open circles).

5. Summary and conclusions

The present analysis is based on the first times-series observations of dissolved oxygen collected from a moored array in a marine environment. Despite its obvious brevity, the oxygen record is of sufficient quality to support continued development of fluorescence-based moored sensors for long-term measurement of in situ water property variability. More specifically, the

application of various analytical techniques to the combined temperature, salinity and oxygen records indicates that data obtained from the oxygen sensor are qualitatively as good as those from the standard conductivity sensor used on Aanderaa RCM4 current meters. Additional field trials are needed to confirm the long-term stability of the sensor and to improve its high-frequency response.

The six-day time series from 100 m depth within the main oxycline in Saanich Inlet reveals that dissolved oxygen fluctuations are predominantly of semidiurnal period and of opposite phase to temperature and salinity fluctuations over the observed frequency bands. There is also evidence for longer term variations in dissolved oxygen which are not accompanied by corresponding variations in temperature, salinity or horizontal velocity. Except for higher frequencies, spectra of temperature, salinity and oxygen within the range $f \leq \omega \leq N$ attenuate approximately as ω^{-2} suggestive of vertical displacements associated with isotropic internal gravity wave activity.

Although possible problems of long-term stability and biofouling still need to be addressed, the oxygen probe provides accurate observations of dissolved oxygen concentrations in the moored configuration and would appear to be ideal for long-term monitoring in regions of significant oxygen variability. Studies of upwelling along continental margins and the intrusion of relatively dense water into coastal fjords are among a variety of investigations that would benefit from the availability of a moorable dissolved oxygen probe. The present device could also be used with a CTD for profiling purposes. To this end, development work is underway to shorten the time response and decrease the noise level of the sensor.

Acknowledgments. We wish to thank the various people who contributed to the project; special thanks to Walter Cretney, who provided scientific insight into the instrument development, and to Peter Berrang whose enthusiastic support ensured that the instrument was built. Donna LePape assisted with the instrument development and Randy Kashino helped collect the water property data. Additional assistance in instrument development was provided by Brian Fowler and Chuck Spencer. Mooring operations were conducted by Al Stickland and Reg Bigham with assistance from the Institute of Ocean Sciences Ship's Division. Data were processed by Dennis Francis and Joe Linguanti. All diagrams were drawn by Patricia Kimber. Sus Tabata reviewed the manuscript. The development of the fluorescence-based oxygen sensor was supported financially by the Department of Supply and Services Canada, the Department of Fisheries and Oceans Canada and the Natural Sciences and Engineering Research Council of Canada.

REFERENCES

Anderson, J. S., and A. H. Devol, 1973: Deep-water renewal in Saanich Inlet, an intermittantly anoxic basin. *Estuarine Coastal Mar. Sci.*, **1**, 1–10.

Bergman, I., 1968: Rapid-response atmospheric oxygen monitor based on fluorescence quenching. *Nature*, **218**, 396 pp.

Berlman, I. B., 1971: *Handbook of Fluorescence Spectra of Aromatic Molecules.* Academic Press, 2nd ed., 473 pp.

Canadian Hydrographic Service, 1986: *Canadian Tide and Current Tables,* Vol. 5. Department of Fisheries and Oceans, Ottawa, 85 pp.

Garrett, C. J. R., and W. H. Munk, 1972: Space-time scales of internal waves. *Geophys. Fluid Dyn.*, **2**, 225–264.

——, and ——, 1975: Space-time scales of internal waves: A progress report. *Geophys. Fluid Res.*, **80**, 291–297.

Gehrich, J. L., D. W. Lubbers, N. Opitz, D. R. Hansmann, W. W. Miller, J. K. Tusa and M. Yafuso, 1986: Optical fluorescence and its application to intravascular blood gas monitoring system. *IEEE Trans. Biomed. Eng.*, BME-33, **2**, 117–132.

Herlinveaux, R. H., 1962: Oceanography of Saanich Inlet in Vancouver Island, British Columbia. *J. Fish. Res. Board Can.*, **19**, 1–37.

Hitchman, M. L., 1978: *Measurement of Dissolved Oxygen.* Wiley and Sons, 255 pp.

Kautsky, H., 1939: Quenching of luminescence by oxygen. *Trans. Faraday Soc.*, **35**, 216–219.

Langdon, C., 1984: Dissolved oxygen monitoring system using a pulsed electrode: Design, performance and evaluation. *Deep-Sea Res.*, **31**, 1357–1367.

McFarlane, R., and W. Liese, 1984: A report on the feasibility of developing a fibre optics dissolved oxygen sensor for oceanographic applications, Seastar Instruments Ltd., File S-6-1, 35 pp.

——, and M. C. Hamilton, 1987: A fluorescence based dissolved oxygen sensor. *Proc. Fourth Int. Symp. on Optical and Optoelectronic Applied Science and Engineering,* SPIE, 324–330.

Peterson, J. I., R. V. Fitzgerland and D. K. Buckhold, 1984: Fiber optic probe for in vivo measurement of oxygen partial pressure. *Ann. Chem.*, **56**, 62–67.

Pickard, G. L., 1975: Annual and larger term variations of the deep-water properties in the coastal waters of southern British Columbia. *J. Fish. Res. Board Can.*, **32**, 1561–1587.

Strickland, J. D. H., and T. R. Parsons, 1968: A practical handbook of seawater analysis. *Bull. Fish. Res. Board Can.*, **167**, 311 pp.

Stucchi, D. J., and L. F. Giovando, 1984: Deep water renewal in Saanich Inlet, B.C. *Proc. Multidisciplinary Symp. on Saanich Inlet, 2nd February, 1983.* S. K. Juniper and P. O. Brinkhurst, Eds., [*Can. Tech. Rep. Hydrogr. Ocean Sci.*: **38**], 7–15.

Wolfbeis, O. S., H. E. Posch and H. W. Kroneis, 1985: Fiber optic fluorosensor for determination of Halothane and/or oxygen. *Ann. Chem.*, **57**, 2556–2561.

Zhujun, Z., and W. R. Seitz, 1986. Optical sensor for oxygen based on immobilized hemoglobin. *Ann. Chem.*, **58**, 220–222.